Hydrogen centers and the conductivity of In_{2}O_{3} single crystals

Weikai Yin, Kirby Smithe, Philip Weiser, Michael Stavola, W. Beall Fowler, Lynn Boatner, Stephen J. Pearton, David C. Hays, and Sandro G. Koch

Phys. Rev. B **91**, 075208 — Published 24 February 2015

DOI: 10.1103/PhysRevB.91.075208

Hydrogen centers and the conductivity of In_2O_3 single crystals

Weikai Yin,[1] Kirby Smithe,[1] Philip Weiser,[1] Michael Stavola,[1,*] W. Beall Fowler,[1] Lynn Boatner,[2] Stephen J. Pearton,[3] David C. Hays,[3] and Sandro G. Koch[4]

[1]Department of Physics and the Sherman Fairchild Laboratory, Lehigh University, Bethlehem, Pennsylvania 18015, USA

[2]Oak Ridge National Laboratory, Materials Science and Technology Division, Oak Ridge, Tennessee 37831, USA

[3]Department of Materials Science and Engineering, University of Florida, Gainesville, Florida 32611, USA

[4]Technische Universität Dresden, 01062 Dresden, Germany

Abstract

A series of IR absorption experiments and complementary theory have been performed to determine the properties of OH and OD centers in In_2O_3 single crystals. Annealing In_2O_3 samples in H_2 or D_2 at temperatures near 450°C produces an n-type layer ≈0.06 mm thick with an n-type doping of 1.6×10^{19} cm^{-3}. The resulting free-carrier absorption is correlated with an OH center with a vibrational frequency of 3306 cm^{-1} that we associate with interstitial H^+. Additional O-H (O-D) vibrational lines are assigned to metastable configurations of the interstitial H^+ (D^+) center and complexes of H (D) with In vacancies. Unlike other oxides studied recently where H trapped at an oxygen vacancy is the dominant shallow donor (ZnO and SnO_2, for example), interstitial H^+ is found to be the dominant H-related shallow donor in In_2O_3.

I. INTRODUCTION

The transparent conducting oxides (TCO's) combine high electrical conductivity with transparency in the visible region of the spectrum.[1-4] In spite of their decades-long applications as transparent electrical contacts, in circuitry, and as coatings for low-emissivity windows, the mechanisms for the conductivity of TCO's are only now being clarified. Oxygen vacancies and cation interstitials traditionally have been invoked as the causes of conductivity. In recent studies, however, hydrogen impurities have been found to be the dominant shallow donors in several important cases.[5-10]

In_2O_3, a prototypical transparent conducting oxide, has the cubic bixbyite structure with a conventional unit cell that contains 80 atoms.[11] The oxygen sites are all equivalent. There are two inequivalent In sites, In(1) (25%) and In(2) (75%). The In(1) site is more symmetrical and has six equivalent In-O bonds. The In(2) site is less symmetrical and has three inequivalent pairs of In-O bonds with no linear O-In-O bonds. Ref. 12 provides further details regarding the bixbyite structure.

The role played by hydrogen impurities in the conductivity of indium oxide (In_2O_3) has been controversial. Some studies, based on the effect of oxygen partial pressure in growth or annealing environments, argue that oxygen vacancies are the cause of the conductivity of In_2O_3.[13-15] However, there is a growing body of theoretical and experimental work which finds that hydrogen centers can be important shallow donors in In_2O_3. Muon-spin-resonance experiments find that implanted muons, whose properties mimic those of hydrogen, form shallow donors in In_2O_3.[16] In_2O_3 thin films containing hydrogen show n-type conductivity with high mobility,[17] and theory finds that interstitial hydrogen (H_i^+) and hydrogen trapped at an oxygen vacancy (H_O^+) are shallow donors that can give rise to n-type conductivity or compensate acceptors in In_2O_3.[12]

In the present paper, infrared (IR) spectroscopy, Hall effect measurements, and theory are used to investigate the microscopic properties of hydrogen centers in In_2O_3 single crystals and the role that hydrogen plays in giving rise to conductivity.

II. EXPERIMENT

The In_2O_3 samples used in our experiments were bulk single crystals grown by the flux method[18] at the Oak Ridge National Laboratory (ORNL) and had typical dimensions of 3 x 3 x 1 mm^3. Most as-grown samples were pale yellow in color. The properties of similar In_2O_3 crystals, also grown at ORNL, have been reported recently.[19] The as-grown crystals were found to have a high resistivity (2 x 10^5 Ω-cm). A few additional In_2O_3 samples that were gray in color were also examined in our experiments.

To introduce additional hydrogen or deuterium, In_2O_3 samples were placed in sealed quartz ampoules filled with H_2 or D_2 gas (2/3 atm at room temperature), annealed at elevated temperature, and cooled to room temperature by withdrawing the sealed ampoule from the furnace. These anneals in H_2 or D_2 produced an opaque layer of In at the sample surface that could be removed by soaking in an 1:4 mixture of HNO_3/H_2O.

IR absorption spectra were measured with a Bomem DA.3 Fourier transform infrared spectrometer. O-H and O-D vibrational modes were measured for In_2O_3 samples held at 4.2 or 77 K with an InSb detector. Samples were cooled with a Helitran continuous-flow cryostat. The absorption due to free carriers[20] was measured for the In_2O_3 samples to provide a contact-free method to probe the free-carrier concentration that is convenient for annealing experiments.

Raman measurements were performed in a 90° geometry using the frequency doubled 532 nm line of a Nd:YVO_4 laser for excitation. The scattered light was analyzed using a single grating spectrometer with a cooled Si CCD detector array.

To probe the reactions and thermal stabilities of the various hydrogen-containing centers, annealing treatments were performed in a tube furnace with a flowing He ambient.

III. EXPERIMENTAL RESULTS

As-grown In_2O_3 single crystals that were initially pale yellow in color showed no substantial IR absorption arising from free carriers. Samples were annealed in H_2 or D_2 ambients to introduce H or D. For long annealing treatments in H_2 or D_2 (>1 hr) at temperatures above 500°C, the samples became dark in color and were opaque in the mid-IR spectral region of interest here. We selected temperatures near 450 to 500°C and H_2 or D_2 treatment times near 30 to 60 min to produce hydrogenated (or deuterated) samples that were deep red in color and sufficiently transparent for IR measurements.

A. Free-carrier absorption and O-H vibrational lines

The introduction of H or D into In_2O_3 produced the broad absorption characteristic of free carriers that increases in strength at low frequency [Fig. 1(a)].[20] Furthermore, several O-H stretching modes were also introduced [Fig. 1(b)].

Figure 2 shows IR spectra (4.2 K) for In_2O_3 samples that had been treated in D_2 or H_2. The upper spectrum in Fig. 2(a) for the deuterated sample shows 9 resolved IR lines. The upper spectrum in Fig. 2(b) for the hydrogenated sample also shows 9 IR lines. The dominant IR lines are at 3306 cm^{-1} for H and at 2464 cm^{-1} for D. The line at 2464 cm^{-1} has a partially resolved shoulder at 2469 cm^{-1}. The line at 3306 cm^{-1} is slightly asymmetric, suggesting the presence of an unresolved line at 3316 cm^{-1} that is the isotopic partner of the shoulder at 2469 cm^{-1}. [The lower spectrum shown in Fig. 2(a) for a hydrogenated sample is featureless in this region. The

lower spectrum in Fig. 2(b) shows the spectral features arising from H that typically remained in samples even after treatment in a D_2 ambient.]

The vibrational frequencies of these lines are listed in Table I. The ratios of the corresponding line frequencies in the H and D spectra are near 1.35, consistent with vibrational modes of H or D bonded to a light element like oxygen.[21] The high frequency of the vibrational lines and the value of the isotopic ratio r lead to the assignment of the lines listed in Table I to O-H and O-D stretching modes.

B. Annealing and thinning experiments

Figure 1 shows that both the free-carrier absorption and the 3306 cm^{-1} O-H line are annealed away together for annealing temperatures in the 500 to 600°C range. Similar annealing experiments were performed for a sample treated in a D_2 ambient (Fig. 3). (Samples annealed in H_2 or D_2 were red in color following treatment and returned to pale yellow after the H or D had been annealed away.) The correlation between the free-carrier absorption and the intensities of the O-H and O-D lines at 3306 and 2464 cm^{-1} in annealing experiments leads us to assign these vibrational lines to interstitial H^+ and D^+ shallow-donor centers predicted by theory.[12]

Experiments were performed to investigate how far H had penetrated into an In_2O_3 sample following a hydrogenation treatment in H_2. An as-grown sample was initially annealed at 1000°C for 30 min in flowing He to eliminate any H that might be present. There was no IR absorption observed that might be due to free carriers or O-H centers following this treatment [see the bottom spectra in Figs. 4(a) and 4(b) labeled H-free].] This sample was then annealed in an H_2 ambient at 450°C for 30 min.

Layers were then successively removed from the sample surfaces by lapping and polishing. The sample thickness was measured with a micrometer as the sample was thinned. IR spectra

[Figs. 4(a) and 4(b)] were measured as layers were removed to monitor both the free-carrier and O-H vibrational absorption. The total thickness removed from the two surfaces after each thinning step is indicated in Fig. 4 in units mm.

The decrease in both the free-carrier absorption and the area of the 3306 cm^{-1} line intensities are plotted together in Fig. 5. The free-carrier absorption and 3306 cm^{-1} O-H line are removed together as the sample is thinned. The hydrogenated layer is removed from the near-surface region of the sample when 0.06 mm is lapped from the surface of the In_2O_3 sample. These experiments show that both the free carriers and OH centers arise from a thin layer near the sample surface, further supporting the assignment of the 3306 cm^{-1} O-H line to an interstitial H^+ shallow donor that gives rise to the free-carrier absorption seen for H treated samples. An indiffusion depth of 0.06 mm is consistent with a H diffusivity in In_2O_3 of 5 x 10^{-9} cm^2/s at 450°C.

C. Calibration of IR lines

Infrared absorption and Hall effect measurements were performed for the same deuterated In_2O_3 sample to approximately calibrate the strengths of the 3306 and 2464 cm^{-1} vibrational absorption lines assigned to shallow donor centers. An In_2O_3 sample was annealed (60 min) in a D_2 ambient at 450°C to produce OD shallow donors. IR absorption measurements were made to determine the integrated areas of the O-D and O-H lines at 2464 and 3306 cm^{-1}. Hall effect measurements yielded a sheet carrier concentration of 1.6 x 10^{17} cm^{-2} for this D-treated sample. Following the Hall measurements, this sample was thinned in steps to remove the O-H and O-D line absorption and also the free carrier absorption, similar to the results shown in Fig. 4, to determine the thickness of the doped layer. The total thickness of the doped layer (sum of front and back surfaces) was found to be 0.10 mm. The local carrier concentration in a doped layer is, therefore, ~1.6 x 10^{19} cm^{-3}. (This result is not the upper limit for the free-carrier density

that can be produced by hydrogenation. Treating samples at higher temperatures or for longer times produced substantially stronger free-carrier absorption that made the samples opaque.)

The concentration N of defects (cm^{-3}) is proportional to the integrated absorption coefficient for the corresponding vibrational absorption line and is given by,[22]

$$N = (m \eta c^2 / \pi q_{eff}^2) \int \alpha \, d\sigma \qquad (1)$$

Here, m is the mass of the oscillating impurity, H or D; η is the refractive index [taken to be η = 2.0 for In_2O_3 (refs. 1 and 11)]; α is the absorption coefficient; σ is the frequency in wavenumbers; and q_{eff} is an effective oscillating charge, given in terms of the electron charge in esu. [Eq. (1) is written in CGS units to be consistent with the absorption coefficient, conventionally expressed in units of cm^{-1}, and the frequency in wavenumber units, also cm^{-1}.]

Our results yield an effect charge of q_{eff} = 0.26 e for the 3306 and 2464 cm^{-1} vibrational absorption lines assigned to the interstitial hydrogen and deuterium shallow donors in In_2O_3. This result for q_{eff} is similar to that found previously for the O-H line at 3611 cm^{-1} in ZnO, whose effective charge is 0.28 e.[23]

D. H_O shallow donors?

Most of the conductivity changes produced by the introduction of H (or D) into In_2O_3 in our experiments can be explained by an interstitial H^+ (or D^+) center that acts as a shallow donor. However, there is some experimental evidence for “hidden hydrogen” that does not give rise to O-H vibrational absorption but that remains electrically active, nonetheless. The data in Fig. 1 show that for a hydrogenated sample annealed at 100°C, the free-carrier absorption remained unchanged while the 3306 cm^{-1} O-H line was decreased in intensity by ~40%. Annealing at higher temperatures caused the intensity of the O-H absorption to recover. This result suggests

that interstitial H^+ can be partially converted by annealing near 100°C into an electrically active H center that gives no observable O-H vibrational absorption. The shallow donor center with H trapped at an oxygen vacancy (H_O^+) predicted by theory[12] is a candidate for such a defect. The vibrational absorption arising from the H_O^+ center is expected to lie at a frequency too low to be observed by IR transmission measurements,[7,24] as predicted by theory to be discussed below (Table II). (Figure 3 shows a similar result for an In_2O_3 sample containing D when it was annealed near 150°C. The O-D line intensity is decreased by ~40% while the free-carrier absorption remains unchanged, suggesting conversions between interstitial D^+ and D_O^+ shallow donors.)

Interstitial H^+ and H_O^+ shallow donor centers have been found to coexist in other oxides, ZnO and SnO_2, for example.[23,25,26] In these cases, H_O^+ is more thermally stable than interstitial H^+ and is the dominant donor in the material. Our results for In_2O_3 indicate that, in this case, it is interstitial H^+ that is the dominant H-related shallow donor.

E. Other IR absorption lines

A number of O-H and O-D absorption lines in addition to the lines at 3306 and 2464 cm^{-1} (Table I) were seen in spectra measured for as-grown samples of In_2O_3 and for samples treated in H_2 or D_2.[27] These lines might be due to metastable interstitial H configurations[12] or H associated with a native defect such as the In vacancy.[28] These additional vibrational lines appeared in different samples with different relative intensities, depending on the sample treatment, with one exception. The O-D lines at 2469 and 2516 cm^{-1} (Fig. 6) were introduced together and were annealed away together in our experiments. (Of the corresponding O-H lines at 3316 and 3398 cm^{-1}, only one is resolved, making these O-H lines difficult to study.)

Both H and D were introduced together into In_2O_3 samples to investigate whether or not defects containing more than one H (or D) atom could be produced. In spite of several attempts

to diffuse H and D into In_2O_3 layers of similar thickness, no new absorption lines that might arise from centers containing both H and D were found.[22] Implications of this result are discussed in Sec. IV.

F. Other shallow donors and deep compensating centers

While most of the samples we studied were pale yellow in color, a few as-grown samples had different colors. IR spectra are shown in Fig. 7 for an as-grown sample that was gray in color. In this case, several O-H absorption lines are seen along with substantial free-carrier absorption.

Annealing experiments (Fig. 7) found that the free-carrier absorption in this gray-colored sample was thermally stable for an annealing temperature of 700°C where H centers and their associated O-H lines are annealed away. These annealing results indicate that this gray-colored sample contains thermally stable shallow donors other than interstitial hydrogen.

The as-grown In_2O_3 samples we studied, whether pale yellow in color or gray, showed weak absorption at 3306 cm^{-1} in addition to other O-H absorption lines, similar to the 3306 cm^{-1} line seen in Fig. 7. From the areas of the 3306 cm^{-1} line seen in typical as-grown samples and the calibration of this absorption given in Eq. (1), we estimate an interstitial hydrogen donor concentration between $2x10^{16}$ and 10^{17} cm^{-3} that is due to hydrogen that was introduced unintentionally into In_2O_3 samples during the growth process that was carried out in the air.

Samples that are pale yellow in color did not show substantial free-carrier absorption in our experiments, and similar samples, also grown at Oak Ridge, were found in another study to have high resistivity.[19] Our infrared results for the concentrations of H_i^+ shallow donors in as-grown In_2O_3 samples suggest that for such samples to have high resistivities, they must contain compensating defects - also at the ~10^{17} cm^{-3} level.

The concentrations of hydrogen (or deuterium) shallow donors introduced intentionally into thin layers by annealing in an H_2 (or D_2) ambient at 500°C in our experiments are near 10^{19} cm^{-3} and would dominate the n-type doping in these layers, even if these In_2O_3 samples contained compensating centers at the 10^{17} cm^{-3} level.

We attempted to produce free carriers in In_2O_3 samples by annealing in reducing ambients that did not include hydrogen. Annealing samples in flowing He at 800°C did not produce free-carrier absorption that is at all comparable to that shown in Figs. 1 and 3. Similarly, annealing In_2O_3 samples in a flowing CO ambient at 700°C for 2 hrs did not produce substantial free-carrier absorption.

IV. DEFECT MODELING

The complex structure of In_2O_3 requires a careful and detailed analysis of possible defect models. This situation has been discussed extensively and relevant calculations have been reported in Refs. 12 and 28. We have carried out similar calculations with the CRYSTAL06 code[29] using DFT with a gradient-corrected approximation to the exchange-correlation functional (Becke's B3LYP potential[30] as implemented in CRYSTAL06 with 20 % exact exchange and Lee-Yang-Parr correlation[31]). The H defect calculations were carried out in a periodic supercell containing 80 host atoms plus one or more H impurities, with computed lattice constants. A 2 x 2 x 2 k-point mesh of Monkhorst-Pack[32] type was used. The SCF energy convergence criterion was 10^{-7} Ha except for vibrational calculations, where 10^{-10} or 10^{-11} Ha was used. Gaussian basis functions were of the type 311p(1)for hydrogen[33] and 8411 for oxygen[34]. For indium[35] the calculations utilized a Barthelet-Durand[36] pseudopotential, with corresponding basis functions.

Where our results correspond to those of Refs. 12 and 28, there is for the most part agreement. Ref. 12 predicts that the four inequivalent BC configurations for H^+ are unstable. Of

the four antibonding (AB) configurations, our results (Table II) and those of Ref. 12 predict that the structure shown in Fig. 8(a) is lowest in energy, while the remaining three configurations shown in Fig. 8(b) are metastable. Thus the O-H (O-D) line at 3306 (2464) cm^{-1} is assigned to the lowest energy antibonding configuration shown in Fig. 8(a).

Assuming a reservoir of molecular O_2, our calculations predict that H_i^+ is energetically favored over H^+ substituted for a neutral oxygen by 4.3 eV,[37] while given an H^+ and an existing O vacancy, the substitutional configuration is favored over separated H_i^+ and O vacancy by 2 eV. And indeed, our experimental results show that H_i^+ is the dominant H-related shallow donor in In_2O_3. Furthermore, our results also suggest that H_O^+ may coexist with H_i^+ following annealing treatments near 100°C. Except in this brief annealing window between 100 to 200°C, H_i^+ can explain the free-carrier absorption we have observed as well as the shallow donors from which it arises without the need for invoking additional shallow H centers. This is different from the situation for H in ZnO and SnO_2 where H_O^+ has been found to be the more thermally stable H-containing shallow center and H_i^+ is only marginally stable at room temperature.

There are several lines in the O-H and O-D spectra in addition to the 3306 and 2464 cm^{-1} lines attributed to the lowest energy interstitial H and D centers. Candidates for these additional lines include the metastable antibonding configurations for H_i^+ shown in Fig. 8(b), centers with H in V_{In},[28] and hydrogen defects that contain more than one H atom.

The metastable AB configurations have predicted vibrational frequencies that are substantially higher than the 3306 cm^{-1} line (Table II) and are, therefore, candidates for the H lines observed between 3375 and 3425 cm^{-1}. The large differences in predicted frequencies arise from the inequivalences in geometry of the different interstitial sites, which in turn, lead to differences in the O-H bond lengths and strengths. These configurations, however, are at least 0.5 eV higher in energy than the stable configuration, so their population is open to question.

There are two inequivalent In sites, In(1) and In(2), or 8b and 24d, respectively, in Wyckoff notation. One of the 24d sites for H in an In vacancy (24d eq:S in the notation of Ref. 28) has

the lowest energy and also has the lowest predicted vibrational frequency of the three possible sites. Ref. 28 predicts this frequency to be 13 cm^{-1} higher than that of H_i^+, while we predict it to be 90 cm^{-1} higher (Table II). Nevertheless, this defect is perhaps a candidate for one of the vibrational lines seen between 3225 and 3290 cm^{-1}

Other, metastable V_{In}-H configurations have predicted vibrational frequencies approximately 200 cm^{-1} higher than H_i^+ and are also candidates for the vibrational lines observed between 3375 and 3425 cm^{-1}. Again, the circumstances in which these metastable sites are populated are not clear.

We also consider configurations with more than one H or D atom. The vibrational lines at 2469 and 2521 cm^{-1} are seen together in the spectra that we have measured for different deuterium-introduction treatments and following annealing treatments. These results suggest that both lines arise from the same D-containing center. If this were the case, one might expect the lines to shift if one of the D is replaced by an H. This, however, has not been observed in experiments on mixed H-D samples.

To consider this further, we have carried out calculations for two H in an In vacancy. There are three pairs of equivalent sites at the In(2) vacancy. We find that if the two H are attached to an equivalent pair, even though the coupling is weak, the degeneracy of these sites predicts that lines for H-D will be displaced by ~ 10 to 15 cm^{-1} from those predicted for H-H or D-D. As noted, this is not seen experimentally. However, if the two H are attached to an inequivalent pair, the new lines predicted for H-D will be displaced from the H-H or D-D lines by less than 1 cm^{-1}, i.e., by a value too small to be resolved. And, the lowest-energy situation does involve hydrogens on *inequivalent* sites. Again, site population issues become critical; if, for example, the sites are randomly populated by two H, there is only a 20% probability that they will be on equivalent sites. Therefore, the possibility of two (or more) H in an In vacancy remains as a possibility. But alternatively, one line of the pair of lines could be an O-D stretching mode and

the second could be due to the 2nd harmonic mode of an O-D wag mode associated with the same defect and with an intensity that is strengthened by Fermi resonance.[22]

V. CONCLUSIONS

The effect that hydrogen impurities have on the conductivity of In_2O_3 single crystals has been studied by IR spectroscopy and theory. Annealing In_2O_3 crystals in an H_2 or D_2 ambient at temperatures near 450°C was found to produce a thin conducting layer near the sample surface with a thickness ≈ 0.06 mm and with a carrier concentration determined by Hall measurements to be 1.6×10^{19} cm^{-3}. An OH vibrational line at 3306 cm^{-1} has been assigned to the interstitial H shallow-donor center that is responsible for the hydrogen-related conductivity. The corresponding D_i center has an OD line at 2464 cm^{-1}. The H_i center was found to be thermally stable up to ≈ 500°C.

Several additional OH lines were produced by the treatment of In_2O_3 in H. Additional configurations for interstitial H with higher formation energies or defects with H trapped by In vacancies that have been investigated by theory are candidates for these OH lines. A comparison of experiment with the relative vibrational frequencies for these H-containing defects predicted by theory (Ref. 28 and Table II) suggests specific assignments.

Investigations of hydrogen shallow-donor centers in other conducting oxides studied recently, ZnO and SnO_2 for example,[23,25,26] find that H_i is only marginally stable at room temperature and H_O is a more thermally stable donor that dominates the n-type conductivity of hydrogenated samples of these materials stored for substantial times at room temperature. Our experimental results and complementary theory show that the conductivity produced by the thermal treatment of In_2O_3 in hydrogen can be explained primarily by a thermally stable H_i center, consistent with theoretical predictions that H_O has a higher formation energy.

VI. ACKNOWLEDGMENTS

The work at Lehigh University was supported by NSF Grant No. DMR 1160756 and NSF REU Program Grant No. PHY-0849416. M.S. is grateful for support for visits to Dresden from the Humboldt Foundation. Research at the Oak Ridge National Laboratory for one author (L. A. B.) is sponsored by the U.S. Department of Energy, Basic Energy Sciences, Materials Science and Technology Division. The work at UF was partially supported by NSF Grant No. EPMD 1159682.

Table I. Vibrational frequencies of O-H (O-D) modes seen for hydrogenated (deuterated) In_2O_3 single crystals. A possible shoulder giving rise to the asymmetry of the 3306 cm^{-1} line is unresolved.

ω_H (cm^{-1})	ω_D (cm^{-1})	r
3225	2407	1.340
3271	2436	1.343
3290	2455	1.340
3306	2464	1.342
3316 (unres.)	2469	1.343
3357	2494	1.346
3373	2504	1.347
3390	2516	1.347
3398	2521	1.348
3411	2530	1.348

Table II. Calculated vibrational frequencies and formation energies relative to the most stable configurations for H centers in In_2O_3. Defect labeling follows that of Refs. 12 and 28. Frequencies for H_i and V_{In}-H centers include the effect of anharmonicity. (The anharmonic corrections that yield the listed values of ω_H are shown in parentheses.) The results shown for H_O and D_O are harmonic frequencies.

Defect	Energy (eV)	ω_H ($\Delta\omega_H$) (cm^{-1})	ω_D (cm^{-1})
$H_i^+(AB_{01})$	0	2931 (301)	2193
$H_i^+(AB_{02})$	0.51	3125 (249)	2325
$H_i^+(AB_{03})$	0.82	3283 (297)	2449
$H_i^+(AB_{04})$	0.82	3453 (209)	2555
$[V_{In}(24d)\text{-}H]^{-2}$ (eq:S)	0	3026 (201)	2253
$[V_{In}(24d)\text{-}H]^{-2}$ (ax)	0.56	3340 (207)	2473
$[V_{In}(24d)\text{-}H]^{-2}$ (eq:L)	0.58	3313 (254)	2453
$[V_{In}(8b)\text{-}H]^{-2}$		3434 (211)	2540
H_O		800	566
$[V_{In}(24d)\text{-}2H]^{-1}$		range from 3150 to 3525	range from 2225 to 2500

References

1. H. L. Hartnagel, A. L. Dawar, A. K. Jain, C. Jagadish, *Semiconducting Transparent Thin Films* (Institute of Physics, London, 1995).
2. A. Facchetti and T. Marks (eds.) *Transparent Electronics: From Synthesis to Applications* (Wiley, New York, 2010).
3. See the special issue of the Journal of Physics: Condensed Matter, Semiconducting Oxides, edited by R. Catlow and A. Walsh, J. Phys. Condens. Matter **23**, 330301 (2011).
4. *Oxide Semiconductors*, edited by B.G. Svensson, S.J. Pearton, and C. Jagadish (Academic Press, San Diego, 2013).
5. C.G. Van de Walle, Phys. Rev. Lett. **85**, 1012 (2000).
6. Ç. Kiliç and A. Zunger, Appl. Phys. Lett. **81**, 73 (2002).
7. A. Janotti and C.G. Van de Walle, Nature Materials **6**, 44 (2006).
8. P.D.C. King and T.D. Veal, J. Phys. Condens. Matter **23**, 334214 (2011).
9. M.D. McCluskey, M. C. Tarun, and S. T. Teklemichael, J. Mater. Res. **17**, 2190 (2012).
10. H. Li and J. Robertson, J. Appl. Phys. **115**, 203708 (2014).
11. I. Hamberg and C. G. Granqvist, J. Appl. Phys. **60**, R123 (1986).
12. S. Limpijumnong, P. Reunchan, A. Janotti, and C. G. Van de Walle, Phys. Rev. B **80**, 193202 (2009).
13. S. Lee and D. C. Paine, Appl. Phys. Lett. **102**, 052101 (2013).
14. J. H. W. De Wit, J. Sol. State Chem. **13**, 192 (1975).
15. J. H. W. De Wit, G. Van Unen, and M. Lahey, J. Phys. Chem. Solids **38**, 819 (1977).
16. P.D.C. King, R.L. Lichti, Y.G. Celebi, J.M. Gil, R.C. Vilão, H.V. Alberto, J. Piroto Durte, D.J. Payne, R.G. Egdell, I. McKenzie, C.F. McConville, S.F.J. Cox, and T.D. Veal, Phys. Rev. B **80**, 081201(R) (2009).
17. T. Koida, H. Fujiwara, and M. Kondo, Jpn. J. Appl. Phys. **46**, L685 (2007).

18. J. P. Remeika and E. G. Spencer, J. Appl. Phys. **35**, 2803 (1964).

19. D. R. Hagleitner, M. Menhart, P. Jacobson, S. Blomberg, K. Schulte, E. Lundgren, M. Kubicek, J. Fleig, F. Kubel, C. Puls, A. Limbeck, H. Hutter, L. A. Boatner, M. Schmid, and U. Diebold, Phys. Rev. B **85**, 115441 (2012).

20. P. Y. Yu and M. Cardona, *Fundamentals of Semiconductors, Physics and Materials Properties* (Springer, Berlin, 2010), 4th ed.

21. M. Wöhlecke and L. Kovács, Critical Reviews in Solid State and Materials Sciences **26**, 1 (2001).

22. M. Stavola, in *Identification of Defects in Semiconductors*, edited by M. Stavola (Academic Press, San Diego, 1999), Chap. 3, p. 153.

23. E. V. Lavrov, F. Herklotz, and J. Weber, Phys. Rev. B **79**, 165210 (2009).

24. S.G. Koch, E.V. Lavrov, and J. Weber, Phys. Rev. Lett. **108**, 165501 (2012).

25. W.M. Hlaing Oo, S. Tabatabaei, M.D. McCluskey, J.B. Varley, A. Janotti, and C.G. Van de Walle, Phys. Rev. B **82**, 193201 (2010).

26. F. Bekisli, M. Stavola, W.B. Fowler, L. Boatner, E. Spahr, and G. Lüpke, Phys. Rev. B **84**, 035213 (2011).

27. In_2O_3 samples that had been deliberately hydrogenated or deuterated by an anneal in H_2 or D_2 gas at 500°C were found to be opaque in the spectral region with a frequency near 2000 cm^{-1} and below. However, following annealing treatments at temperatures near 400°C that reduced the free carrier concentration, an additional strong IR absorption line emerged at 1890 cm^{-1} as the sample increased in transparency. We found that this line showed no H vs D isotope effect. Raman measurements made for our In_2O_3 samples in their as-grown state showed a strong line at 630 cm^{-1}, in agreement with a previous Raman study of In_2O_3 powder [G. P. Schwartz, W. A. Sunder, and J. E. Griffins, J. Electrochem. Soc. **129**, 1361 (1982)]. We attribute the 1890 cm^{-1} line to the third harmonic of an In_2O_3 lattice phonon with frequency 630 cm^{-1} that has been seen with Raman spectroscopy.

28. J. B. Varley, H. Peelaers, A. Janotti, and C. G. Van de Walle, J. Phys. Condens. Matter **23**, 334212 (2011).
29. R. Dovesi, V. R. Saunders, C. Roetti, R. Orlando, C. M. Zicovich-Wilson, F. Pascale, B. Civalleri, K. Doll, N. M. Harrison, I. J. Bush, Ph. D'Arco, M. Llunell, *Crystal06 User's Manual*, University of Torino, Torino, 2006.
30. A. D. Becke, J. Chem. Phys. **98**, 5648 (1993).
31. C. Lee, W. Yang, and R. G. Parr, Phys. Rev. B **37**, 785 (1988).
32. H. J. Monkhorst and J. D. Pack, Phys. Rev. B **13**, 5188 (1976).
33. R. Krishnan, J. S. Binkley, R. Seeger, and J. A. Pople, J. Chem. Phys. **72**, 650 (1980).
34. J. E. Jaffe and A. C. Hess, Phys. Rev. B **48**, 7903-7909 (1993).
35. M. Causà, R. Dovesi, and C. Roetti, Phys. Rev. B **43**, 11937 (1991).
36. P. Durand and J. C. Barthelat, Theor. Chim. Acta **38**, 283 (1975); J. C. Barthelat and P. Durand, Gazz. Chim. Ital. **108**, 225 (1978).
37. Following the procedure of Ref. 12, this would correspond to 0.64 eV in an In-rich situation.

Figure Captions

FIG. 1. A selection of IR absorption spectra (T = 4.2 K, resolution = 1 cm^{-1}) for an In_2O_3 sample that initially had been hydrogenated by an anneal (30 min) in an H_2 ambient at 500°C. The sample was then annealed sequentially in flowing He at the temperatures shown in °C. (a) The absorption due to free carriers. (b) The IR absorption lines in the O-H stretching region. These spectra were baseline corrected to remove the contribution from free carriers.

FIG. 2. IR absorption spectra (4.2 K, resolution = 1 cm^{-1}) for In_2O_3 samples containing D and H. Spectra were baseline corrected to remove the contribution from free carriers. The sample for the upper spectrum in (a) had been deuterated by annealing in a D_2 ambient (60 min) at 500°C. It was then annealed in flowing He at 550°C to increase its transparency and to produce the O-D lines that are shown. The sample for the upper spectrum in (b) had been hydrogenated by annealing (30 min) in an H_2 ambient at 500°C and subsequently annealed (30 min) at 550°C. [The lower spectrum in (a) shows the D-stretching region for a hydrogenated sample and the lower spectrum in (b) shows the H-stretching region for a deuterated sample.]

FIG. 3. A selection of IR absorption spectra (T = 77 K, resolution = 1 cm^{-1}) for an In_2O_3 sample that initially had been annealed (60 min) in flowing He at 850°C to remove any hydrogen that might have been present and was subsequently deuterated by an anneal (30 min) in an D_2 ambient at 500°C. The sample was then annealed sequentially in a flowing He at the temperatures shown in °C. (a) The absorption due to free carriers. (Free carrier absorption spectra measured following anneals from 50 to 250°C are indistinguishable from the results shown for the D-treated sample and also following the anneal at 200°C.) (b) The IR absorption lines in the O-D stretching region. These spectra were baseline corrected to remove the contribution from free carriers.

FIG. 4. A selection of IR absorption spectra (T = 77 K, resolution = 1 cm^{-1}) for an In_2O_3 sample that initially had been annealed (30 min) in flowing He at 1000°C to remove any hydrogen that might have been present and was subsequently hydrogenated by an anneal (30 min) in an H_2 ambient at 450°C. The sample was then sequentially thinned by lapping and polishing the front and back surfaces. The thickness removed following each thinning step (both sides) is shown in mm. (a) shows free-carrier absorption spectra for the H-treated sample and for the sample following thinning. (b) shows baseline-corrected IR spectra of the O-H absorption lines.

FIG. 5. Strength of free-carrier absorption and O-H vibrational absorption for the In_2O_3 sample whose IR data are shown in Fig. 4 as a function of thickness removed from the sample. The left scale (filled circles) shows the difference in the free-carrier absorption at 2500 and 4000 cm^{-1} for each thickness removed. The right scale (open circles) shows the integrated absorbance for the 3306 cm^{-1} O-H stretching line assigned to the interstitial H^+ shallow donor for each thickness removed.

FIG. 6. IR absorption spectrum (T = 4.2 K, resolution = 1 cm^{-1}) for an In_2O_3 sample deuterated by an anneal (60 min) in a D_2 ambient at 500°C.

FIG. 7. A selection of IR absorption spectra (T = 77 K, resolution = 1 cm^{-1}) for an as-grown In_2O_3 sample that was grey in color. The sample was annealed sequentially in flowing He at the temperatures shown in °C. (a) The absorption due to free carriers. (b) The IR absorption lines in the O-H stretching region. These spectra were baseline corrected to remove the contribution from free carriers.

FIG. 8. Defect models. (a) The lowest energy antibonding configuration (AB_{01}) for H_i^+. (b) Metastable H_i^+ antibonding configurations (AB_{02} to AB_{04}). Defect labeling follows Ref. 12. (c) Lowest energy configuration for $[V_{In}(24d)\text{-}H]^{2-}$. Larger (blue) atoms represent O, smaller (black) atoms represent In, and the smallest (red) atom is H. This was constructed by MOLDRAW (P. Ugliengo, Torino 2006, available at http://www.moldraw.unito.it) and POV-Ray (http://povray.org).

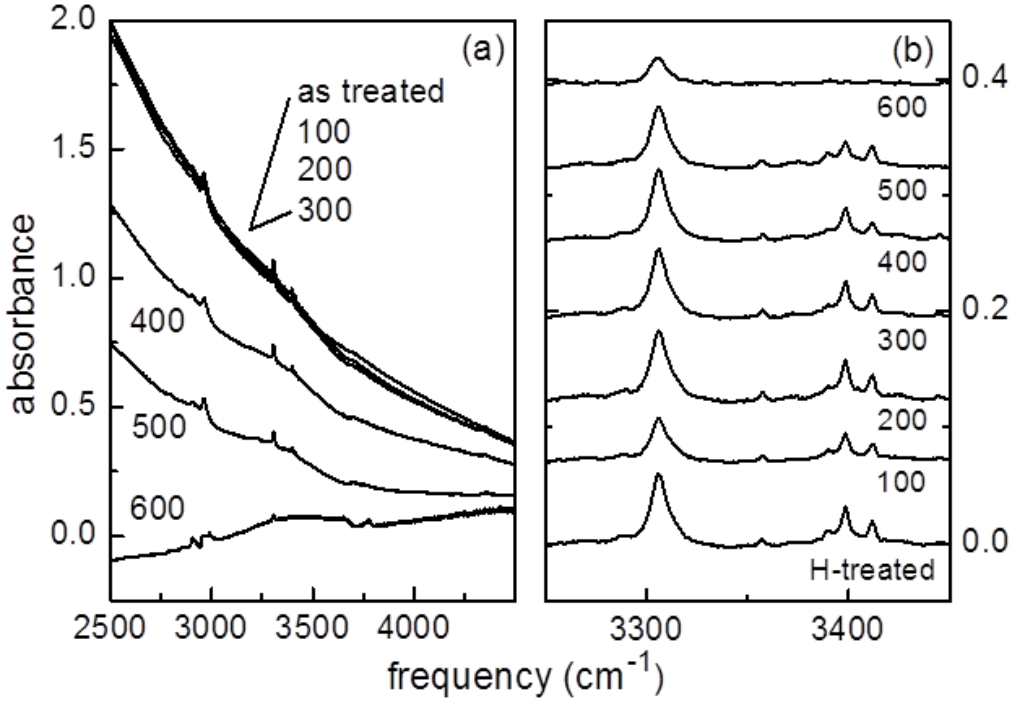
(a)
(b)
as treated
100
200
300
400
500
600
H-treated
absorbance
frequency (cm-1)
2.0
1.5
1.0
0.5
0.0
0.4
0.2
0.0
2500
3000
3500
4000
3300
3400

Fig. 1

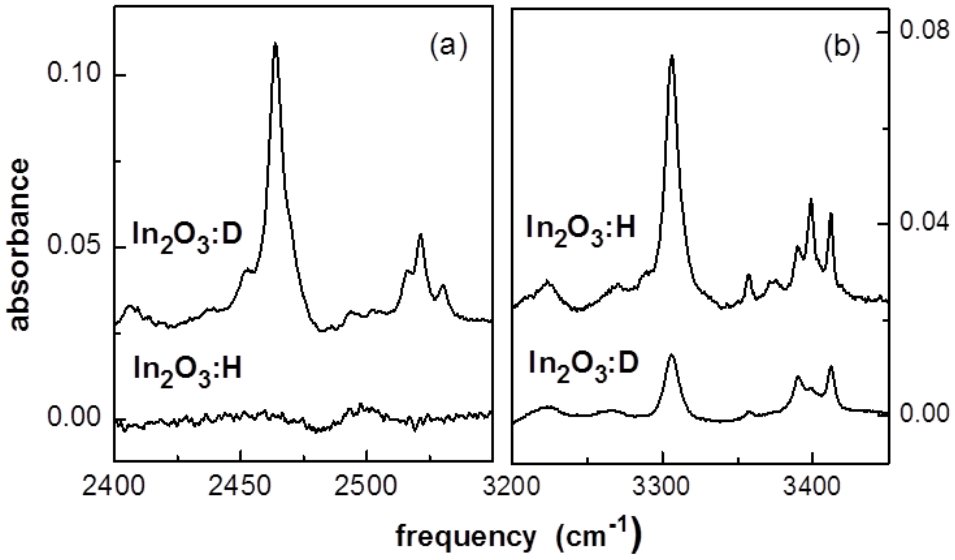
(a)
(b)
In2O3:D
In2O3:H
In2O3:H
In2O3:D
absorbance
frequency (cm-1)
0.10
0.05
0.00
0.08
0.04
0.00
2400
2450
2500
3200
3300
3400

Fig. 2

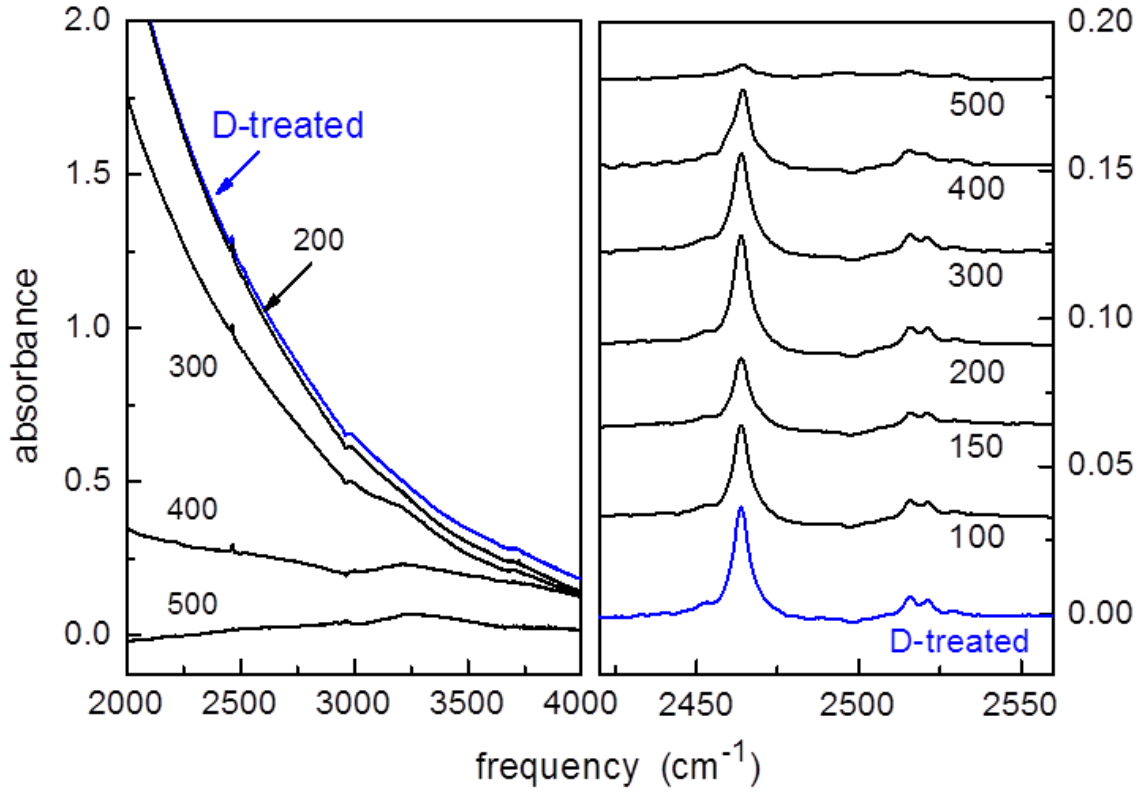
2.0
1.5
1.0
0.5
0.0
absorbance
D-treated
200
300
400
500
2000
2500
3000
3500
4000
2450
2500
2550
0.20
0.15
0.10
0.05
0.00
500
400
300
200
150
100
D-treated
frequency (cm-1)

Fig. 3

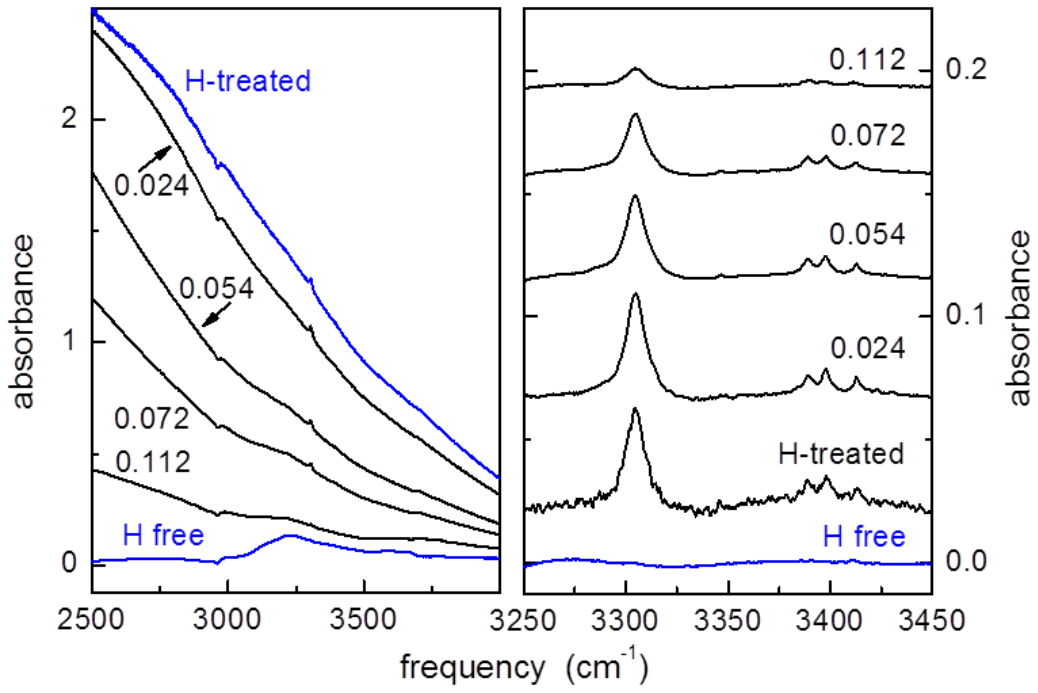
H-treated
0.024
0.054
0.072
0.112
H free
2
1
0
absorbance
2500
3000
3500
3250
3300
3350
3400
3450
0.112
0.072
0.054
0.024
H-treated
H free
0.2
0.1
0.0
absorbance
frequency (cm-1)

Fig. 4

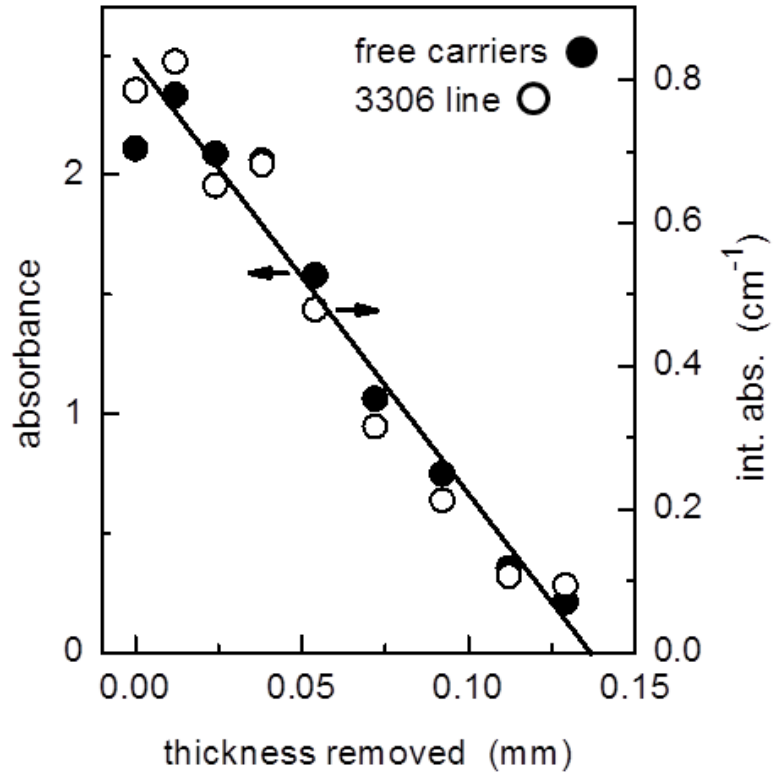
free carriers
3306 line
absorbance
int. abs. (cm-1)
thickness removed (mm)
0
1
2
0.0
0.2
0.4
0.6
0.8
0.00
0.05
0.10
0.15

Fig. 5

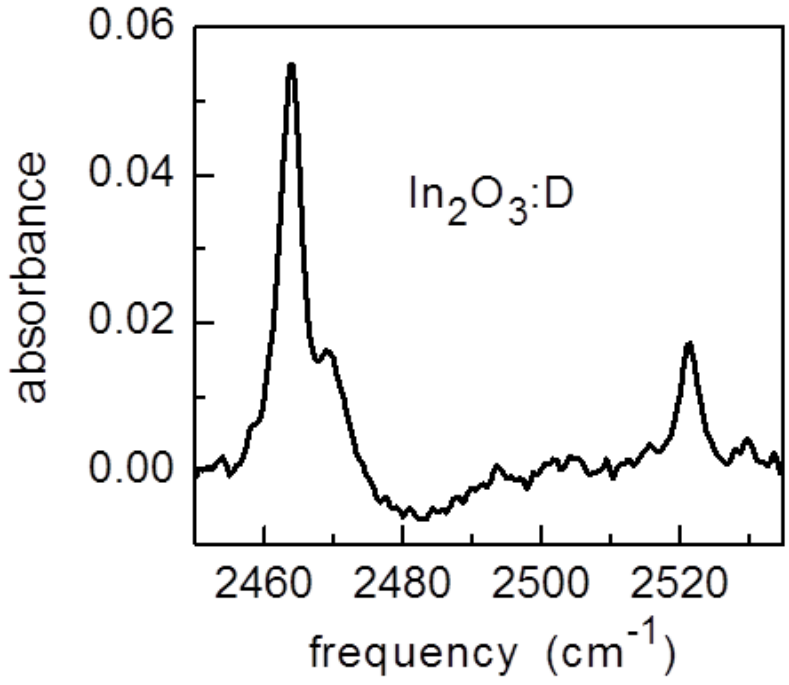
In2O3:D
absorbance
frequency (cm-1)
0.00
0.02
0.04
0.06
2460
2480
2500
2520

Fig. 6

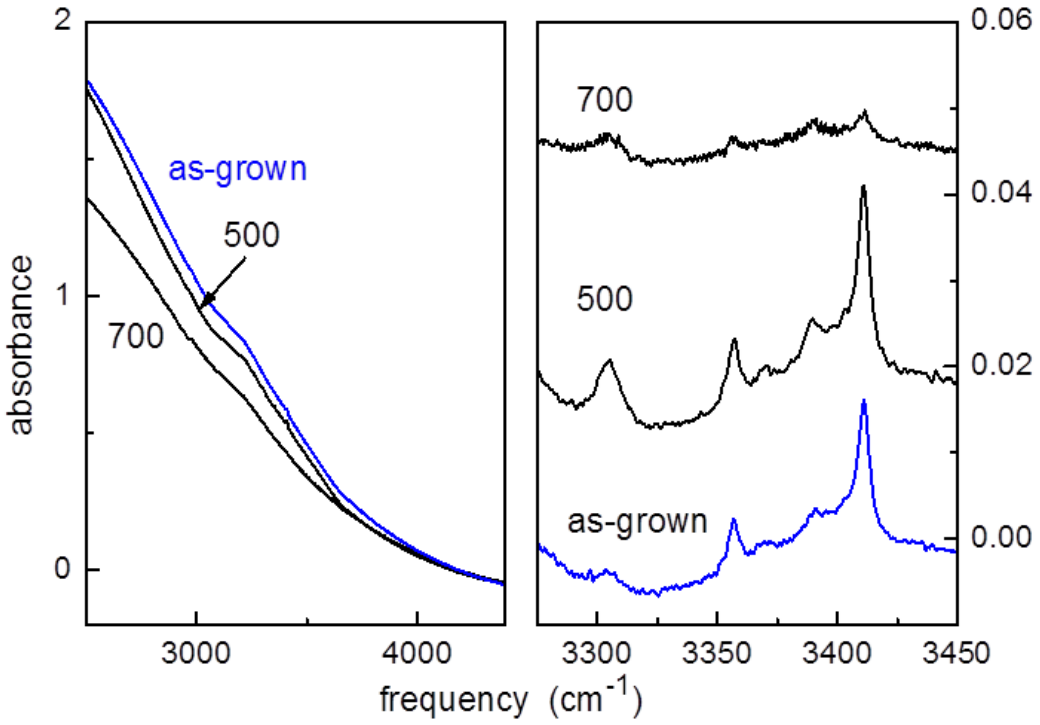
2
1
0
absorbance
as-grown
500
700
3000
4000
0.06
0.04
0.02
0.00
700
500
as-grown
3300
3350
3400
3450
frequency (cm-1)

Fig. 7

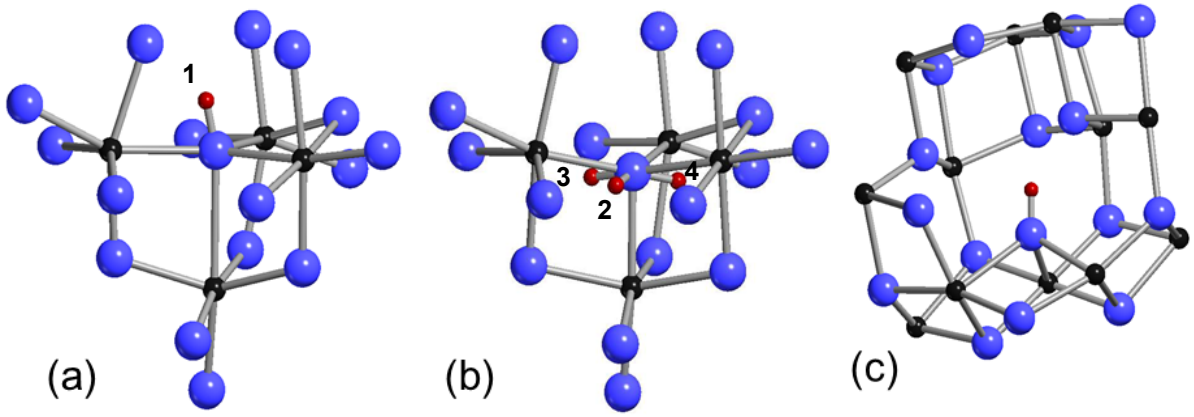
1
(a)
3
2
4
(b)
(c)

Fig. 8